SciMedCentral

Journal of Cancer Biology & Research

Research Article

Osteopontin Delocalization by Applied Low Intensity Static Magnetic Field in Cultured Human Glioblastoma Cells

Seung Chan Kim[1]* and Beom Jin Kim[2]

[1]*Medical School and College of Medicine, Yonsei University, Republic of Korea*
[2]*Department of Mathematics, Yonsei University, Republic of Korea*

Abstract

Osteopontin (OPN) is a protein associated with several cellular processes, including development, carcinogenesis, and adhesion. The U87 and U251 glioblastoma multiforme cell line is a model for fast-growing malignant tumors. Taking advantage of the relatively fast growing speed of this cell line, we investigated the subcellular relocalization of proteins as an indicator of time-dependent effects following a treatment with static magnetic field (2000 ± 600 Gauss). OPN, which plays an important role in adhesion and mitosis, was transported from the perinucleus to the cytoplasm upon static magnetic stimulation ($p = 0.0217$). Similarly, tubulin gamma complex associated protein 3 (GCP3) was dispersed. Tunneling electron microscopy indicated that the membranous structures had changed. Our findings suggest that static magnetic fields induce the dispersion of cytoplasmic intracellular proteins such as OPN and GCP3.

***Corresponding author**

Seung Chan Kim, Medical School College of Medicine, Department of Integrated OMICS for Biomedical Sciences (World Class University Program), the School of Graduate Studies, Yonsei University, Yonsei-ro 50, Shinchon-dong, Seodaemoon-gu, Seoul, Republic of Korea, Tel: 82-2-6245-2835; Fax: 82-2-6245-2835; Email: synedit@gmail.com

Submitted: 20 February 2017

Accepted: 27 March 2017

Published: 29 March 2017

Keywords

- Glioblastoma
- Proliferation
- Static magnetic field
- Alteration of molecular patterns
- Osteopontin

ABBREVIATIONS

OPN: Osteopontin; TUBGCP3/GCP3: Tubulin, Gamma Complex Protein 3

INTRODUCTION

Glioblastoma is currently treated with surgery, radiotherapy, and chemotherapy [1-3]. Current therapeutic strategies are only effective in less-advanced stages of the disease with a localized tumor mass [4-6]. However, current therapies are not sufficiently effective to cure cancer at an advanced phase [7,8] or with a high rate of recurrence [9-11]. Radiation therapy may also lead to side effects such as decline in immunity [12], the formation of secondary tumors [13], and the alteration of mental abilities. Due to the adverse effects of widely applied established cures, alternative therapies such as drug delivery using specific cancer markers [14-16] and magnetic therapy [17,18] are currently under investigation in clinical research.

OPN is a protein associated with a variety of cellular processes, including development, carcinogenesis, tissue, and adhesion. Localization of additional proteins implicated in nuclear membrane formation, metastasis, and the regulation of cell cycle were investigated to evaluate the effect of static magnetic fields on mitotic activity and physical mechanisms [19]. By assessing the localization of OPN, the effect of magnetic treatment on mitotic activity and physical mechanisms can be evaluated.

Tunneling electron microscopy (TEM) followed by image analysis was performed to confirm the results. Finally, cell mobility was measured to obtain information about the metastatic activity of different glioblastomas after magnetic treatment.

Our study focused on the changes in subcellular localization and in regulatory effects after the exposure of U251 cells to a static magnetic field.

METHODS

Cell lines

Human U87MG and U251MG glioblastoma cells (American Tissue Culture Collection) were cultured in DMEM supplemented with 10% fetal bovine serum, 100 units/mL penicillin, and 100 µg/mL streptomycin at 37°C in a humidified 5% CO_2 and 95% air atmosphere.

Exposure to static magnetic field

A static magnetic field of 1400-2600 Gauss (measured with the GM08 Gaussmeter, Hirst Magnetic instruments Ltd, England) was used for the treatment, which is about 1/5 intensity compared to that of the MRI. The static magnetic field

was exerted by permanent magnets that were attached to the bottom of 24-well and 96-well plates (Figure 1, 1000 Gauss = 0.1 T [Tesla.]). The north (N) and south (S) poles were arranged randomly. The magnets were located at a distance of 0.1-0.3 cm from the cells. The plates were placed on a plastic shelf (75-T) 4.0 ± 0.2 cm above the metal shelf so that the magnetic field of the metal shelf does not influence the cells. Separate incubators were used for culturing the control and treated cells to avoid affecting the control cells by the magnetic field. Cells were incubated for 48 ± 4 hours.

Immunocytochemistry

Localization of OPN was investigated with immunocytochemistry. Before immunostaining, cells cultured in the 24-well plates were exposed either to the N or S pole of the static magnetic field. The cells were washed with phosphate buffered saline (PBS), fixed with 4% paraformaldehyde, permeabilized with 0.1% Triton X-100 in PBS, and blocked with 1% bovine serum albumin in PBS. Cells were incubated with the primary antibody recognizing OPN (Abcam, Cambridge; 1:1000 dilution; polyclonal). The secondary antibody was Cy3-conjugated goat anti-rabbit (Jackson ImmunoResearch, West Grove, PA). Digital images were saved as separate files for each staining and were merged. Tubulin, gamma complex protein 3 (TUBGCP3) was immunostained in the U87 cell line according to a previously reported protocol [20]. Localization of proteins following an exposure to the static magnetic field was evaluated with statistical analysis.

TEM imaging

Samples were embedded into beam capsules in an oven at 60°C for 48 h. Semithin sections at a thickness of 1 μm were prepared, and they were stained with toluidine blue for 2-5 min. Sections were observed using a microscope. Finally, ultrathin sectioning was performed. Sections were stained to increase electrondensity.

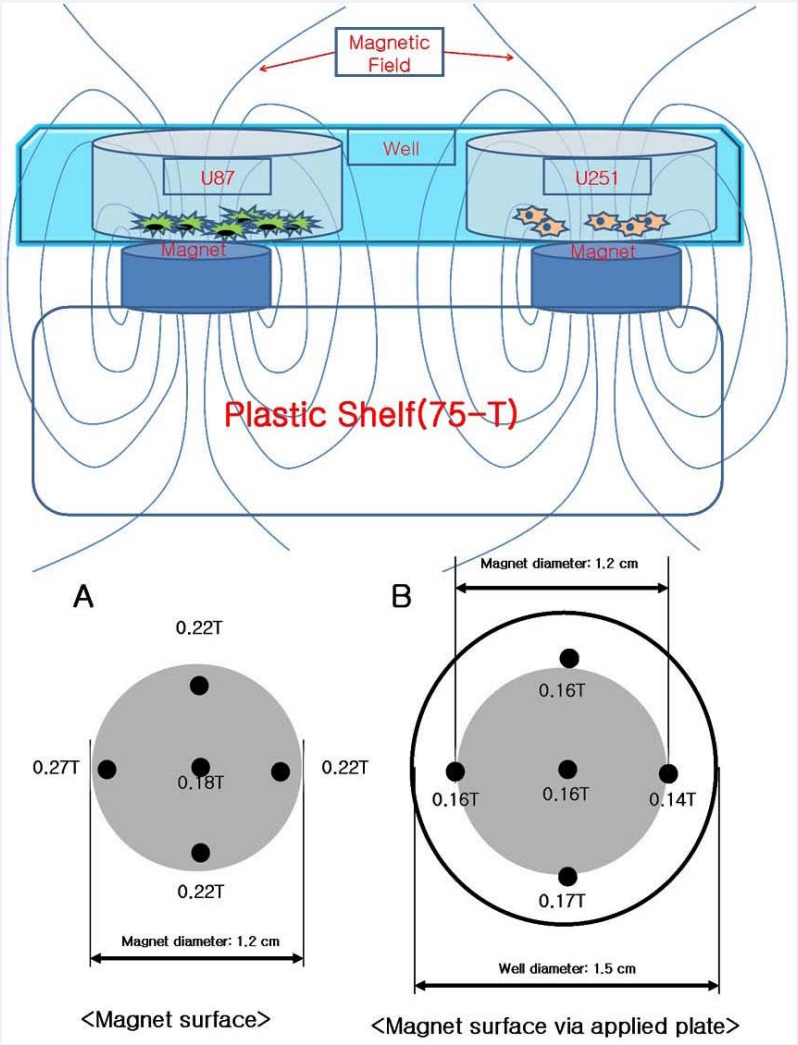

Figure 1 Application of the static magnetic field. Static magnetic fields (1400-2600 Gauss) exerted by permanent magnets were applied to both 24-well and 96-well culture plates by attaching the magnets on the top of plastic shelves (75-T). Plastic shelves were used to minimize the magnetic effect of copper shelves of the incubator. The magnets were at the bottom of the wells at a distance of ~0.3 cm from the cells. The magnetic field intensity was measured without any obstacles present (A) and while the magnet was covered with the cell plate (B).

Migration assay

Cells were plated into 24-well plates to create a confluent monolayer, and the cells were incubated for approximately 6 h at 37°C allowing the cells to adhere to the semi-osmetic pore membrane completely. We adjusted the number of cells required for forming a confluent monolayer depending on both the cell type and the size of the dish. The number of cells that penetrated the substance with a diameter of 8 μm was counted. Cells were investigated with a phase-contrast microscope.

Statistical analysis

Statistical significance of immunocytochemical results regarding the relative localization of proteins was tested with the Pearson's chi-square test. Ratio of the total sum of nuclear area and the total sum of protein-containing area was calculated based on the mathematical boundary in control and treated cells. The null hypothesis stated that the ratio of the magnet-treated group and the control group is 1, and the alternative hypothesis stated that the ratio of the magnet-treated group and the control group is not 1. The null hypothesis was tested with the chi-square test.

RESULTS

Protein expression and immunocytochemistry

We identified significant changes in the protein expression after exposure to the static magnetic field. If the N pole of magnetic fields was applied, OPN was localized in the cytoplasm, whereas in the control cells, OPN was localized in the nucleus (Figure 2). We measured the areas of with OPN and the area of the nuclei using a mathematical calculation based on the identification of the respective boundaries in each individual cell, and we used these data to evaluate the localization of OPN. Sum of the OPN-containing area was divided by the sum of nuclear area in the U251 cell line. U251 cells were chosen for the analysis because the respective areas were more unclear in the U87 cells, and therefore, it was harder to answer whether OPN was localized in the cytoplasm after the magnetic treatment. The area of the OPN-containing region divided by the nuclear area was 2.89 in the control cells, and 5.38 after the magnetic treatment. Cytoplasmic relocalization of OPN after the application of a static magnetic field was statistically significant (chi-square test; $p = 0.0217$). Cells were investigated with confocal microscopy to confirm the changes obtained with fluorescence microscopy (data not shown).

TEM following the application of a static magnetic field

TEM images were obtained and analyzed. In U251 cells treated with magnets irrespective of the poles used (48 hours, 2000 ± 600 Gauss), the contrast of the nuclear membrane boundary was decreased compared with that in the control group. In addition, the subcellular organelles were highly organized and localized

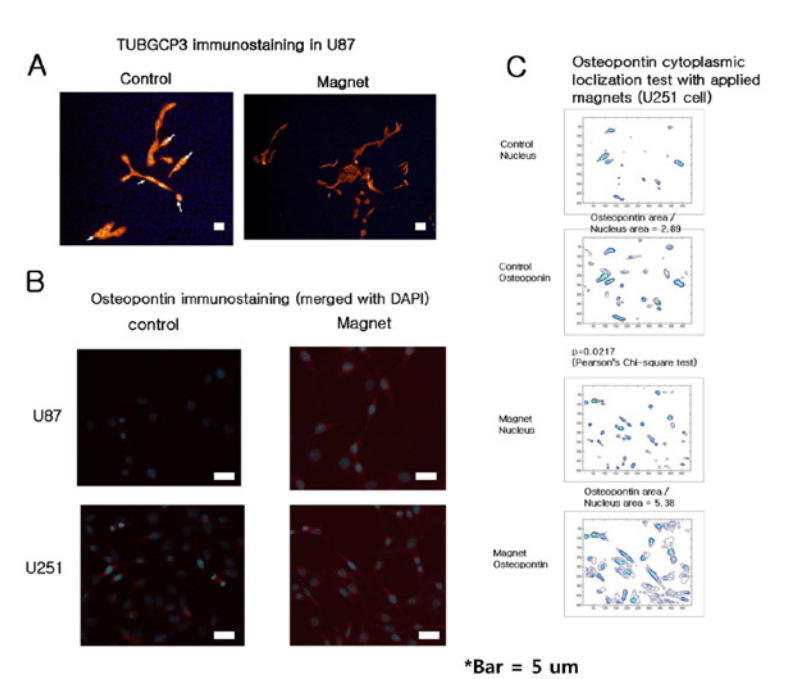

Figure 2 Immunocytochemical staining of TUBGCP3 (A) and OPN (B). Signal of the OPN immunostaining was merged with the signal of the DAPI staining to reveal the relative localization of OPN. Following the application of the static magnetic field, OPN was predominantly localized in the cytoplasm rather than at the nucleus in U251 cells (chi-square test; $p = 0.0217$). Localization was evaluated using a mathematical boundary calculation (C), which measured the total protein-containing area divided by the nuclear area. This relocalization might have a role during mitotic events such as spindle formation. Similar to previous reports, OPN was highly expressed in dividing cells with separating chromosomes (shown in the panel "U251 control"). Tubulin, gamma complex protein 3 (TUBGCP3) was dispersed after the magnetic treatment, whereas its location was structured in control U87 cells.

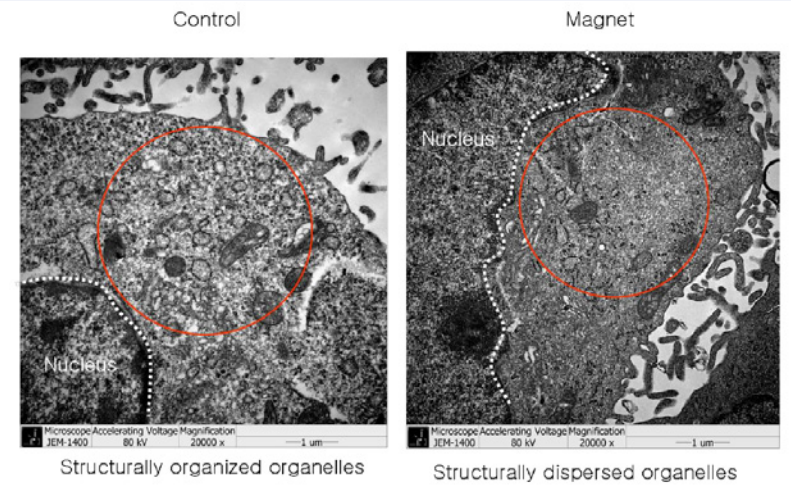

Figure 3 Tunneling electron microscopy and contrast conversion of U251 cells. Proteins were dispersed following the application of a static magnetic field. Additionally, the contrast of the nuclear membrane boundary was decreased in the group treated with a static magnetic field compared with that in the control group.

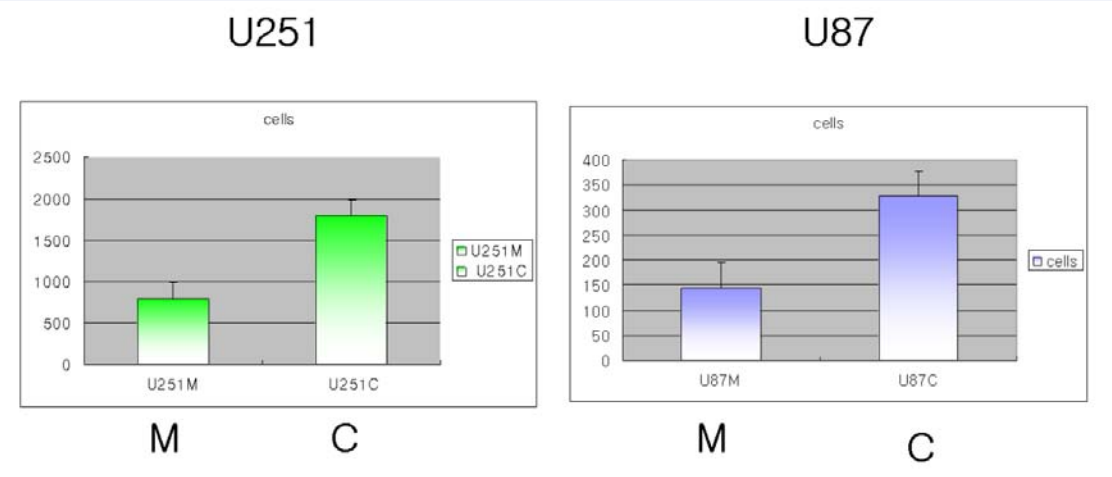

Figure 4 Mobility test cell count after the application of a static magnetic field. Using a substrate with a pore size of 4-8 μm, the mobility of cells decreased after the magnetic treatment. These results correlate with the functional disruption of proteins at the molecular level following the application of a static magnetic field. C: Control; M: Application of a Static Magnetic Field.

in the control cells (Figure 3), but they dispersed following the application of a magnetic field (Figure 3B). Nuclear boundaries become less defined after the magnetic treatment.

Cell mobility of U251 and U87 cells

After the application of a static magnetic field, the monolayer penetrating ability of both U251 and U87 cells decreased. After the control treatment, the total number of cells that crossed the membrane was 1787 and 327 for the U251 and U87 cell lines, respectively. However, after the magnetic treatment, this number decreased to 788 and 145 using the U251 and U87 cell lines, with a cell counting error rate of ± 5% in each cell line (Figure 4).

DISCUSSION

Our study focused on the subcellular localization and regulatory effects of OPN in U251 cells after the application of a static magnetic field. Apoptotic signals, protein expression, or cell mobility changed in parallel. OPN was concentrated in the nuclei of the control cells, whereas it was localized in the cytoplasm upon a treatment with the N pole of a static magnetic field.

OPN localization has an important role in mitosis, although its function is not clearly elucidated yet. In 293 cells, OPN is only detectable within the nucleus during mitosis [21]. Nuclear OPN expression is higher in the G_2/M phase than that in the G_0/G_1 phase. In addition, it is expressed at a significantly higher level in the S phase than in the G_0/G_1 phase according to this study. This might give a possible explanation for the effects of magnets on DNA synthesis in the S phase and on mitotic activity [22].

For enzymes with phosphatase or hydrolytic activities, the activation energy barrier, which is dependent on the dielectric

constant of water molecules, is a major factor that regulates the speed of enzymatic reactions [23,24]. However, the dielectric constant of water molecules is altered by static magnetic fields [25]. Localization of OPN plays a role in the function of polo-like kinase, which oscillates between the polar and mitotic spindles [26]. Therefore, the altered localization of OPN might be related to previous results [20] indicating that disturbances in TUBGCP3 induced by a static magnetic field affect spindle formation. We showed that TUBGCP3 relocalized in U87 cells upon magnetic treatment (Figure 2A), and similar results were shown in C2C12 cells [20].

Several studies reported that the cytoskeleton and other subcellular structures are altered by static magnetic fields [18,20]. Therefore, GCP3 and thus the structure of the cytoskeleton might be altered, which might modulate the rate of proliferation. Furthermore, calcium channels can be altered by static magnetic fields based on a patch clamp study [27]. In accordance with these studies, structural changes were observed with TEM following the application of a static magnetic field. Not only the cytoskeleton, but the nuclear envelope, cytoplasm, and the overall structure of the cell was changed. To understand how these cellular changes are performed, and to clarify the effects of static magnetic fields in cells, further academic studies are warranted.

Our findings provide a new insight into the effects of static magnetic fields on the functional properties of OPN. Structural kinetic studies should be performed with carefully controlled fluorescence resonance energy transfer experiments using the smallest beads possible for low error rates.

ACKNOWLEDGEMENTS

We thank Dr. Wooseok Im for his help in data analysis.

AUTHOR CONTRIBUTIONS

S.C. Kim performed the experiments, analyzed the data, performed the statistical analysis, and wrote the manuscript. B.J. Kim assisted in optimizing the protocols and TEM imaging.

REFERENCES

1. Maher EA, Furnari FB, Bachoo RM, Rowitch DH, Louis DN, Cavenee WK, et al. Malignant glioma: genetics and biology of a grave matter. Genes Dev. 2001; 15: 1311-1333.
2. Lacroix M, Abi-Said D, Fourney DR, Gokaslan ZL, Shi W, DeMonte F, et al. A multivariate analysis of 416 patients with glioblastoma multiforme: prognosis, extent of resection, and survival. J Neurosurg. 2001; 95: 190-198.
3. Chen R, Nishimura MC, Bumbaca SM, Kharbanda S, Forrest WF, Kasman IM, et al. A hierarchy of self-renewing tumor-initiating cell types in glioblastoma. Cancer Cell. 2010; 17: 362-375.
4. Chang JE, Khuntia D, Robins HI, Mehta MP. Radiotherapy and radiosensitizers in the treatment of glioblastoma multiforme. Clin Adv Hematol Oncol. 2007; 5: 894-902, 907-915.
5. Patel RR, Mehta MP. Targeted therapy for brain metastases: improving the therapeutic ratio. Clin Cancer Res. 2007; 13: 1675-1683.
6. Byun Y, Thirumamagal BT, Yang W, Eriksson S, Barth RF, Tjarks W. Preparation and biological evaluation of 10B-enriched 3-[5-{2-(2,3-dihydroxyprop-1-yl)-o-carboran-1-yl}pentan-1-yl] thymidine (N5-2OH), a new boron delivery agent for boron neutron capture therapy of brain tumors. J Med Chem. 2006; 49: 5513-5523.
7. Schneider DT, Wessalowski R, Calaminus G, Pape H, Bamberg M, Engert J, et al. Treatment of recurrent malignant sacrococcygeal germ cell tumors: analysis of 22 patients registered in the German protocols MAKEI 83/86, 89, and 96. J Clin Oncol. 2001; 19: 1951-1960.
8. Feelders RA, Hofland LJ, van Aken MO, Neggers SJ, Lamberts SW, de Herder WW, et al. Medical therapy of acromegaly: efficacy and safety of somatostatin analogues. Drugs. 2009; 69: 2207-2226.
9. Sharma DN, Goyal SG, Muzumder S, Haresh KP, Bahl A, Julka PK, et al. Radiation therapy in paediatric gliomas: our institutional experience. Neurol Neurochir Pol. 2010; 44: 28-34.
10. Wen PY. Therapy for recurrent high-grade gliomas: does continuous dose-intense temozolomide have a role? J Clin Oncol. 2010; 28: 1977-1979.
11. Kioi M, Vogel H, Schultz G, Hoffman RM, Harsh GR, Brown JM. Inhibition of vasculogenesis, but not angiogenesis, prevents the recurrence of glioblastoma after irradiation in mice. J Clin Invest. 2010; 120: 694-705.
12. Gridley DS, Pecaut MJ, Nelson GA. Total-body irradiation with high-LET particles: acute and chronic effects on the immune system. Am J Physiol Regul Integr Comp Physiol. 2002; 282: R677-688.
13. Wright JD, St Clair CM, Deutsch I, Burke WM, Gorrochurn P, Sun X, et al. Pelvic radiotherapy and the risk of secondary leukemia and multiple myeloma. Cancer. 2010; 116: 2486-2492.
14. Ast G. Drug-targeting strategies for prostate cancer. Curr Pharm Des. 2003; 9: 455-466.
15. Koshikawa N, Minegishi T, Nabeshima K, Seiki M. Development of a new tracking tool for the human monomeric laminin-gamma 2 chain in vitro and in vivo. Cancer Res. 2008; 68: 530-536.
16. van de Ven AL, Adler-Storthz K, Richards-Kortum R. Delivery of optical contrast agents using Triton-X100, part 2: enhanced mucosal permeation for the detection of cancer biomarkers. J Biomed Opt. 2009; 14: 021013.
17. Dini L, Abbro L. Bioeffects of moderate-intensity static magnetic fields on cell cultures. Micron. 2005; 36: 195-217.
18. Rosen AD, Chastney EE. Effect of long term exposure to 0.5 T static magnetic fields on growth and size of GH3 cells. Bioelectromagnetics. 2009; 30: 114-149.
19. Elgavish A, Prince C, Chang PL, Lloyd K, Lindsey R, Reed R. Osteopontin stimulates a subpopulation of quiescent human prostate epithelial cells with high proliferative potential to divide in vitro. Prostate. 1998; 35: 83-94.
20. Kim S, Im W. Static magnetic fields inhibit proliferation and disperse subcellular localization of gamma complex protein3 in cultured C2C12 myoblast cells. Cell Biochem Biophys. 2010; 57: 1-8.
21. Junaid A, Moon MC, Harding GE, Zahradka P. Osteopontin localizes to the nucleus of 293 cells and associates with polo-like kinase-1. Am J Physiol Cell Physiol. 2007; 292: 919-926.
22. Kizhatil K, Baker SA, Arshavsky VY, Bennett V. Ankyrin-G promotes

cyclic nucleotide-gated channel transport to rod photoreceptor sensory cilia. Science. 2009; 323: 1614-1617.

23. Knowles JR. Enzyme-catalyzed phosphoryl transfer reactions. Annu Rev Biochem. 1980; 49: 877-919.

24. Törnroth-Horsefield S, Neutze R. Opening and closing the metabolite gate. Proc Natl Acad Sci USA. 2008; 105: 19565-19566.

25. Ibrahim IH. Biophysical Properties of Magnetized Distilled Water. Egypt J Sol. 2006; 29: 363-369.

26. Glover DM, Hagan IM, Tavares AA. Polo-like kinases: a team that plays throughout mitosis. Genes Dev. 1998; 12: 3777-3787.

27. Santamaría D, Barrière C, Cerqueira A, Hunt S, Tardy C, Newton K, et al. Cdk1 is sufficient to drive the mammalian cell cycle. Nature. 2007; 448: 811-815.

Cite this article

Kim SC, Kim BJ (2017) Osteopontin Delocalization by Applied Low Intensity Static Magnetic Field in Cultured Human Glioblastoma Cells. J Cancer Biol Res 5(2): 1099.